




A Targeted Bivalent Androgen Receptor Binding Compound for Prostate Cancer Therapy

Shafinaz Chowdhury¹ · Lenore K. Beitel² · Rose Lumbroso¹ · Enrico O. Purisima^{3,4} · Miltiadis Paliouras^{1,5,6}  · Mark Trifiro^{1,5,7}

Received: 9 September 2018 / Accepted: 5 November 2018 / Published online: 18 December 2018
© Springer Science+Business Media, LLC, part of Springer Nature 2018

Abstract

The androgen-directed treatment of prostate cancer (PCa) is fraught with the recurrent profile of failed treatment due to drug resistance and must be addressed if we are to provide an effective therapeutic option. The most singular difficulty in the treatment of PCa is the failure to respond to classical androgen withdrawal or androgen blockade therapy, which often develops as the malignancy incurs genetic alterations and gain-of-function somatic mutations in the androgen receptor (AR). Physical cellular damaging therapeutic agents, such as radiation or activatable heat-generating transducers would circumvent classical “anti-functional” biological resistance, but to become ultimately effective would require directed application modalities. To this end, we have developed a novel AR-directed therapeutic agent by creating bivalent androgen hormone-AF-2 compounds that bind with high affinity to AR within cells. Here, we used molecular modeling and synthetic chemistry to create a number of compounds by conjugating 5 α -dihydrotestosterone (DHT) to various AF-2 motif sequence peptides, through the use of a glycine and other spacer linkers. Our data indicates these compounds will bind to the AR in vitro and that altering the AF-2 peptide composition of the compound does indeed improve affinity for the AR. We also show that many of these bivalent compounds can readily pass through the plasma membrane and effectively compete against androgens alone.

Keywords Androgen receptor · Prostate cancer · Androgen · Bivalent compound · AF-2 domain · Therapeutics · Molecular dynamics simulation

Dr. Miltiadis Paliouras and Dr. Mark Trifiro share senior authorship.

Electronic supplementary material The online version of this article (<https://doi.org/10.1007/s12672-018-0353-6>) contains supplementary material, which is available to authorized users.

✉ Miltiadis Paliouras
miltiadis.paliouras@mcgill.ca

- ¹ Lady Davis Institute for Medical Research – Jewish General Hospital, 3755 Cote-Ste-Catherine Rd., Montreal, QC H3T 1E2, Canada
- ² Montreal Neurological Institute, McGill University, Montreal, QC, Canada
- ³ National Research Council Canada, Montreal, QC, Canada
- ⁴ Department of Biochemistry, McGill University, Montreal, QC, Canada
- ⁵ Division of Experimental Medicine, McGill University, Montreal, QC, Canada
- ⁶ Department of Medicine/Oncology, McGill University, Montreal, QC, Canada
- ⁷ Division of Endocrinology, Jewish General Hospital, Montreal, QC, Canada

Introduction

Prostate cancer (PCa) is the most common male malignancy and second leading cause of cancer deaths among men, with 30 to 40% of patients diagnosed with localized disease eventually develop metastatic disease [1–4]. The androgen receptor (AR), a ligand inducible steroid hormone receptor, is involved in regulation of prostate growth, spermatogenesis, and bone and muscle mass; however, it is the key determinant in the initiation and progression of PCa [5]. Most patients with PCa respond dramatically to antiandrogen therapy; unfortunately, the median duration of response to hormone therapy is usually only 12 to 18 months, with the majority of patients eventually progressing to castration resistant PCa (CRPC) [6, 7].

Members of nuclear receptor (NR) superfamily, including the AR, act as ligand-activated, DNA-binding, transcription regulatory factors. NRs contain three main functional domains: the C-terminal ligand-binding domain (LBD) receives the signal, the central DNA-binding domain (DBD) binds to a response element near the target gene, and the N-terminal

domain (NTD) modulates gene transcription. All NR LBDs share a common three-dimensional structure encompassing 12 α -helices (numbered 1–12) and two small β -sheets [8–10]. NR ligand specificity is achieved mainly by specific interactions between the ligand and the amino acids lining the ligand-binding pocket (LBP) [11]. In response to ligand-binding, NR LBDs undergo conformational changes and helix 12 moves from an extended (open) position to a closed position, thereby sealing the LBP [12]. Repositioning of helix 12 completes the assembly of the activation function (AF-2) domain, which contains a conserved hydrophobic cleft flanked by opposing-charge residues (formed by specific amino acids from helices 3, 4, 5, and 12) [8, 13, 14].

Therapeutic resistance and the realization that prostatic neoplasms could outwit hormonal therapeutics through gain-of-function somatic mutations of the AR is the biggest shortcoming of current androgen/AR-directed therapeutic modalities [15]. Recent documentation of the mutational profile of CRPC, has identified the AR as the most commonly mutated gene [16]. Moreover, the intervention with androgen hormonal therapy in indolent disease has resulted in selection of diagnosis of patients presenting for aggressive disease [17]. Possible mechanisms of antiandrogen resistance in advanced PCa includes the presence of hypersensitive AR activity through AR amplification, overexpression of co-factors, or specific promiscuous somatic mutations. Somatic AR mutations, allow for a variety of other steroid hormones and classical antiandrogens to replace androgens as active ligand and allow continued activation of AR [18–20]. Somatic mutations of the AR, such as Thr877Ala (T877A), Trp741Cys (W741C), and His874Tyr, and their subversive activity in the presence of antiandrogens have been well documented [19, 21, 22]. Furthermore, the somatic mutation, Phe876Leu (F876L) has been identified and found to circumvent the actions of Enzalutamide (MDV-3100), the compound currently used in the treatment of CRPC [23].

Therefore, the acceptance of “watchful waiting” and non-intervention in early disease has led to a greater improvement in deferring more advanced PCa [24–26]. This has resulted in a real need to devise new therapeutics, where the onus is placed on treating early disease to prevent more advanced disease and limit the progression to therapeutic resistance disease. In this paper, we report the design and synthesis of a number of bivalent androgen compounds for efficient targeting of AR. By creating these bivalent androgen-peptide conjugates with a much-enhanced affinity for the AR-AF2 motif as a targeting arm, where effector moieties, such as radioactive agents, cytotoxic drugs, and small de-couplers which can act as prodrugs, can be delivered with no or limited systemic toxicity.

Experimental

Molecular Modeling

The crystal structure of the ligand-binding domain of AR (PDB code 1t7r) was used as the starting point for the modeling study. Structure manipulation and visualization were done in SYBYL 8.0 (Tripos, Inc., St. Louis, MO). In the crystal structure, dihydrotestosterone (DHT) is in the ligand-binding pocket of AR and the FxxLF motif-containing co-activator peptide is bound in the AF-2 pocket. Both N- and C-termini of the AR were modeled in the ionized state. The C-terminus of the co-activator peptide fragment was also modeled in the ionized state. All histidine residues were protonated. Hydrogen atoms were added and the complex was subjected to conjugate gradient energy minimization using a distance-dependent dielectric function ($\epsilon = 4r$) and an 8 Å non-bonded cut-off down to an rms gradient of 0.01 kcal mol⁻¹ Å⁻¹ using the AMBER ff99SB force field [27, 28]. This complex served as the template for the initial design of our bivalent compounds. The resulting complex and other protein-ligand complexes were energy-minimized with the AMBER and GAFF [29] force fields.

Molecular dynamics simulations were carried out using the AMBER suite of programs. Each system was solvated in a truncated octahedron TIP3P water box. The distance between the wall of the box and the closest atom of the solute was 10.0 Å. Na⁺ and Cl⁻ ions were added to produce an ionic strength of 0.15 M and to neutralize the net charge of the complex. Each system was energy-minimized, applying harmonic restraints with force constants of 1 kcal/mol Å² to all non-hydrogen solute atoms, followed by heating from 10 to 150 K over 30 ps in the canonical ensemble (NVT). Heating was continued with harmonic restraints to bring the temperature from 150 to 300 K over 100 ps in the isothermal-isobaric ensemble (NPT) simulation and to adjust the solvent density under 1 atm pressure. The harmonic restraints were then gradually reduced to zero with four rounds of 250 ps NPT simulations. A 50-ns production run was then carried out with snapshots collected every 10 ps. For all simulations, 2 fs time-step and 8 Å non-bonded cutoff were used. The Particle Mesh Ewald (PME) method [30] was used to treat long-range electrostatics, and bond lengths involving bonds to hydrogen atoms were constrained by SHAKE [31]. For simulations containing peptidomimetic linkers, the AMBER force field had to be supplemented with parameters for the unnatural amino acids present.

Chemistry of SPEP Compounds

Preliminary modeling studies suggested the feasibility of extending the N-terminal end of an AF-2 peptide to connect to the 17 β -hydroxy group of DHT through a carbamate linkage.

Although substitutions at 17α [32] and 17β [33] could be found in the literature, we designed and successfully carried out a novel synthetic scheme for introducing such a linker at the 17β -OH position of DHT. AF-2 peptides were synthesized by Fmoc solid-phase chemistry using manual coupling (Fmoc amino acid, 4 equiv.; 2-(H-benzotriazole-1-yl)-1,1,3,3-tetramethyluronium tetrafluoroborate (TBTU), 4 equiv; *N,N*-diisopropylethylamine (DIPEA), 6 equiv) in *N*-methylpyrrolidone. Synthesized peptides were added to the linker in a subsequent reaction. A five-step synthetic procedure of the bivalent androgen-peptide conjugates has been developed. The first step of the five-step synthetic procedure adopted was the formation of the steroidal-chloroformate (A) by reacting 1 equiv (350 μ M) dihydrotestosterone (DHT) with 1.5 equiv triphosgene, and 1 equiv anhydrous pyridine in anhydrous dichloromethane (DCM) for 5 h at room temperature. Subsequently, coupling of 1 equiv (570 μ M) compound A with 1 equiv *t*-butyl-glycine in the presence of 2.5 equiv triethylamine (Et_3N) in acetonitrile (MeCN) was carried out to form a glycine steroid carbamate (B). Finally, the *t*-butyl group was removed from compound C by trifluoroacetic acid (TFA) in dichloromethane. The glycine steroid carbamate was coupled with the peptide attached to the AF-2 motif peptide on solid phase to form compound D. The final step of the synthetic route was the cleavage of compound D from the attached resin, which generates compound E. Spectral analyses (mass spectroscopy, analytical HPLC) were consistent with the desired products (Scheme 1).

Synthesis of the Stapled Peptide

We procured stapled AF-2 peptide from Biopeptide Co. Inc., (San Diego, CA). Synthesis carried out by Fmoc solid-phase chemistry using unnatural amino acid (*S*)-2-(2- β -pentenyl) alanine to replace *i* and *i* + 4 position alanine (A) and glutamine (Q) of AF-2 peptide sequence respectively. The side chains of this unnatural alanine are then cross-linked with an olefinic bond [34].

In Vitro Binding Assays

We have developed an AR expression system for measure binding properties of bivalent androgen derivatives to androgen receptor. We isolated full-length His-tagged human AR from lysed transfected COS-1 cells by using Ni^{2+} -affinity (Ni^{2+} -NTA) chromatography [35]. Briefly, we performed competition binding assays by pre-incubating immobilized His-AR with specific androgen-peptide conjugates, or the DHT control, overnight at 4 °C. The following day, 5 nM [^3H]-Mibolerone (MB, a synthetic nonmetabolizable androgen) and an additional aliquot of each compound are added. Specific [^3H] MB-AR binding is measured after further 2.5 h incubation at 4 °C. The concentrations of compounds required

to inhibit 50% of MB binding (IC_{50}) are determined for these androgen peptide conjugates.

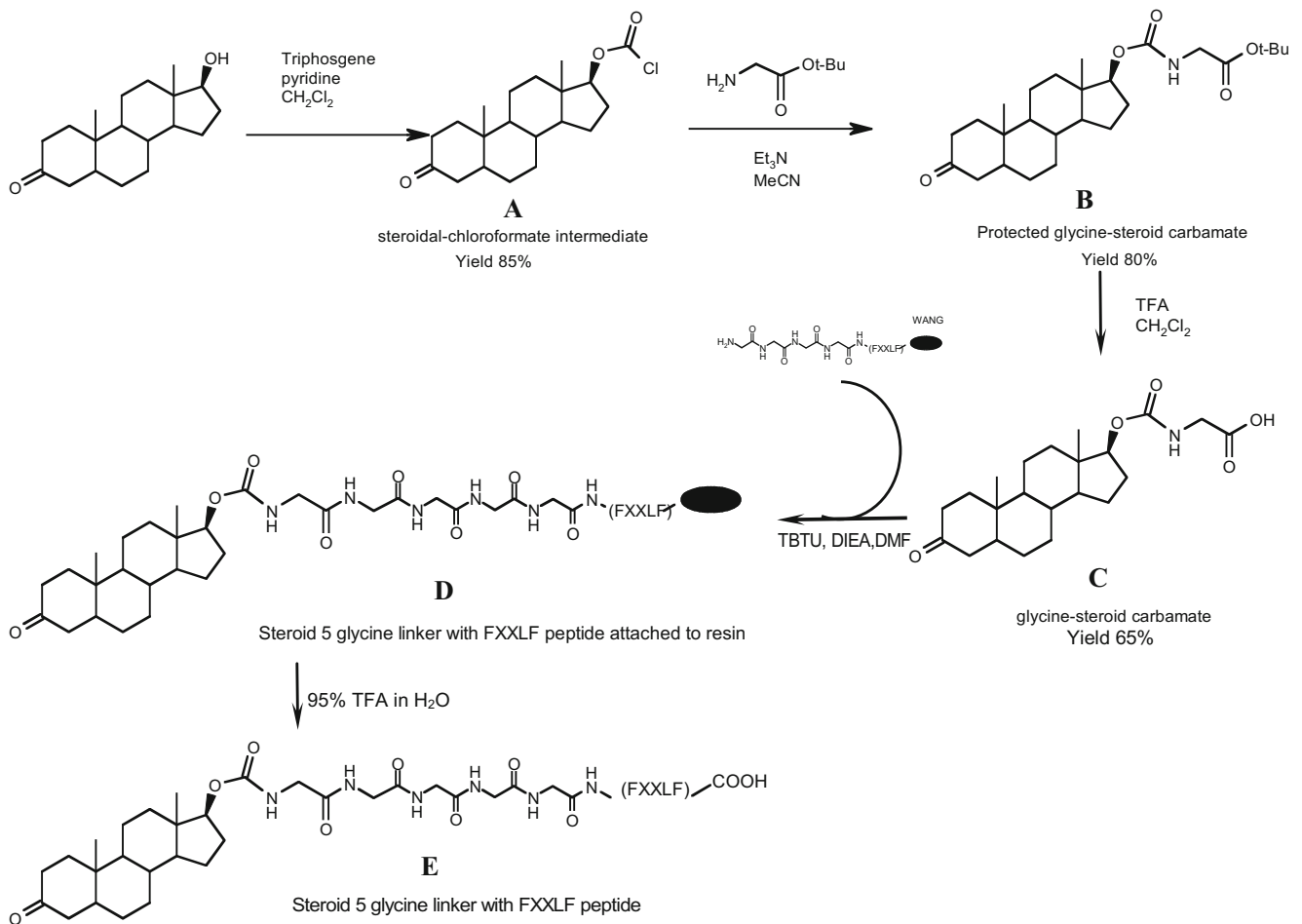
Cell Culture Competition Assays

Competition binding assay was performed by pre-incubating normal genital skin fibroblast (GSF) expressing androgen receptor with synthesized androgen peptide conjugate for 2 h at 37 °C. After the pre-incubation, this compound was incubated with [^3H]-MB at room temperature for 20 min. These cells were then harvested and lysed and the % [^3H]-MB binding in presence of compounds was determined. Finally, we determined percent inhibition of MB binding in genital skin fibroblast (GSF) in presence of specific concentration of compounds (conjugate concentration was 100 nM, except SPEP-24 which was 50 nM).

Results and Discussion

Bi-Valent Androgen Design Strategy

Among all-natural androgens, 5α -dihydrotestosterone (DHT) was selected as a moiety to occupy the androgen-binding pocket. DHT is more selective than testosterone for AR in prostate and has approximately three times greater affinity for the AR than testosterone. DHT acts as the primary androgen in the prostate in adults and like testosterone, it cannot be converted by the enzyme aromatase to estradiol. However, it is almost universal that any steroid manipulation leads to dramatic loss of affinity to the ligand-binding domain (LBD) [36]. To circumvent this problem, we sought to create a bivalent androgen-peptide conjugate where the utilization of two binding sites of AR in the LBD and AF-2 domains results in recuperating the loss of binding affinity associated with the manipulated steroid. A bivalent targeting strategy can exhibit as much as 20- to 50-fold increased affinity [37–40]. Non-steroidal bivalent compounds have also been synthesized for the Estrogen receptor and do show comparable binding to Estradiol, with some compounds' similar effects on breast cancer cell line growth as raloxifene [41, 42]. The AF-2 surface provides binding sites for the recruitment of several co-activators through the co-activators' conserved α -helical LxxLL or FxxLF motifs [43] (Fig. 1a). The AR AF-2 regions exhibit a distinct preference for co-activators with aromatic-rich motifs [8, 44, 45]. Such motifs have been found in N-terminal domain of AR and in an AR cognate family of co-activators that include AR-associated protein (ARA) 54, 55, and 70 [46–48]. The AF-2 region of AR-LBD mediates an androgen-dependent N-terminal/C-terminal (N/C) interaction through an FxxLF motif of the N-terminal AR. This interaction is thought to facilitate and stabilize androgen binding. Each motif forms a two-turn α -helix residing between charged

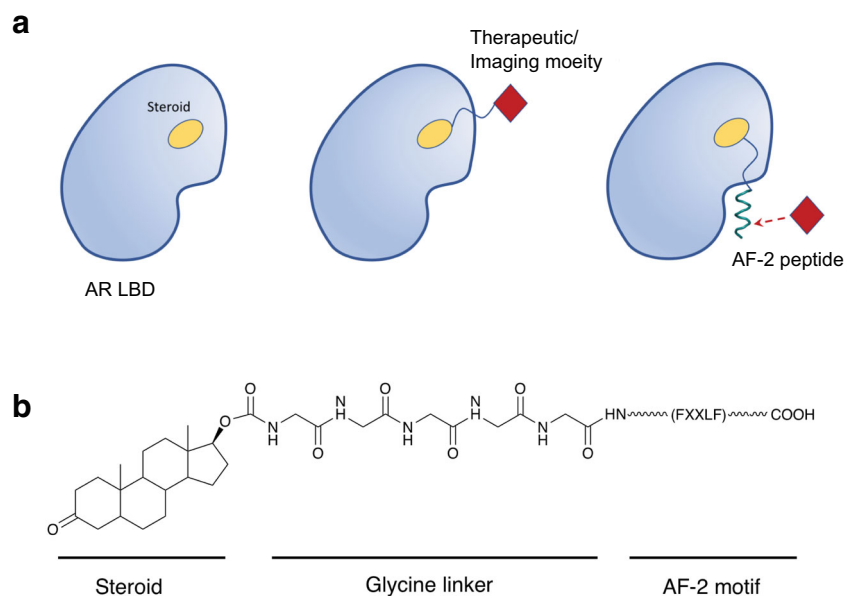


Scheme 1 A five-step synthetic procedure of the bivalent androgen-peptide conjugates

glutamate and lysine residues of AF-2 of AR-LBD. The strategy then was to covalently link the androgen hormone with

AF-2-binding peptides, via a spacer arm, to form our bivalent ligand (Fig. 1b). Aside from contributing to binding affinity,

Fig. 1 Rationale for the androgen-AF-2 bivalent ligand. **a** The androgen is completely buried. Attaching a payload directly to the androgen perturbs the AR structure and androgen binding, resulting in significantly reduced affinity. Linking the androgen to an AF-2 peptide, which binds to the AR surface, recuperates the binding affinity lost resulting from the derivatization of the androgen. The bivalent ligand has an AR binding affinity comparable to that of the androgen and attachment of a payload to the surface-exposed AF-2 peptide is relatively easy without affecting affinity. **b** Components of the androgen-AF-2 bivalent ligand



the AF-2 peptide moiety provides a much more versatile surface-exposed point of attachment than the steroid for a therapeutic abiotic moiety.

Linker and AF-2 Peptide Design

The AR-LBD co-crystal structure shows that the binding sites of the DHT and SSRFESLFAG co-activator peptide (pdb code 1t7r) are 13 Å apart. The androgen-binding pocket is completely buried while the AF-2 binding site is on the surface with no obvious path to connect them. However, inspection of the crystal structure suggested the existence of a nascent channel between the two sites. Molecular modeling suggested that a 5-glycine linker (SPEP-1, Table 1) spanning this channel and conjugating DHT with a co-activator peptide could be accommodated with a modest protein conformational change after energy minimization of the complex (Fig. 2).

To explore the optimal linker length, two other compounds SPEP-2 (Gly₆ linker) and SPEP-3 (Gly₄ linker) were made and tested. All three ligands had an AF-2 FxxLF peptide SSRFGSLFAG [extracted from the crystal structure (1t7r)] with one substitution from FESLF to FGSLF. Of these, SPEP-1 with a Gly₅ linker showed good binding to AR (IC₅₀ 500 nM in an in vitro assay) while SPEP-2 (Gly₄) and SPEP-3 (Gly₆) failed to show any affinity for AR (Table 2). This suggests that Gly₄ is too short to bridge the two sites while the additional two bonds in Gly₆ relative to Gly₅ creates a geometrical constraint on positioning the AF-2 peptide that is incompatible with proper binding.

Using the optimal Gly₅ linker, three other variants containing the FxxLF motif taken from the literature were explored (SPEP-4, SPEP-5, and SPEP-6; Table 1). The three flanking residues on either side of the motif were taken from ARA70 [50]. The SPEP-4 FQNLF motif was derived from the N-terminal domain of AR. SPEP-4 had an IC₅₀ of 300 nM, a modest improvement over SPEP-1 (Table 2). With FAALF (SPEP-5) and FKLLF (SPEP-6), the IC₅₀ improved further to 70 nM and 100 nM, respectively. We have also calculated the inhibitor constant (K_i) for all compounds.

SPEP-9 is a variant of SPEP-5 with an extra-long Gly₁₀ linker. The extra five glycines allow the linker to extend out of the channel with enough flexibility to position the AF-2 peptide with minimal bias from the geometry of exit of the linker from the channel. SPEP-9 has an IC₅₀ of 100 nM, comparable to SPEP-5 (Table 2). This suggests that the Gly₅ linker exits the channel with a geometry that is near optimal for connecting to the preferred binding mode of the AF-2 peptide.

To reduce the number of peptide bonds and the polarity of the linker, we also used γ -Abu-Ahx (γ -4-aminobutanoic acid and 6-aminohexanoic acid) to replace four glycine residues in the linker. G- γ -Abu-Ahx is of similar length to Gly₅ and modeling suggested that it could be accommodated well. SPEP-10 and SPEP-27 are analogs of SPEP-5 and SPEP-6,

respectively, with their Gly₅ linkers replaced by Gly- γ -Abu-Ahx. SPEP-10 and SPEP-27 have IC₅₀s of 25 nM (3-fold improvement) and 50 nM (2-fold improvement), respectively. This shows a clear advantage to using Gly- γ -Abu-Ahx versus Gly₅ as the linker.

Unnatural Amino Acids

To mitigate potential proteolytic degradation of androgen-peptide conjugates, we replaced one or two phenylalanines in the FxxLF motifs of SPEP-5 and SPEP-10 with unnatural amino acids naphthylalanine (NAL) and cyclohexylalanine (CHA) (SPEP-11, SPEP-12, SPEP-13, SPEP-19, SPEP-21, and SPEP-22, Table 1). None of these exhibited improved affinities over their parent compounds (Table 2).

LxxLL Motif

Another series of compounds were designed using sequences from the members of the steroid receptor co-activator p160 SRC family. The p160 SRC family includes SRC-3, SRC-1 and TIF2/GRIP1/SRC-2 co-activators. A conserved feature of these co-activators is an α -helical LxxLL motif or NR box. The androgen receptor recruits SRCs to its ligand-binding domain using these short leucine-rich hydrophobic motifs (LxxLL). We therefore explored replacing phenylalanines with leucines in the AF-2 peptide. SPEP-26 incorporates the LVQLL sequence from SRC-1. The LxxLF motif has not been shown to be a bona fide AF-2 binding motif, thus SPEP-23 and SPEP-24 replace one or both phenylalanines in SPEP-10. Significant improvement in binding affinity was observed for SPEP-24 upon replacing the FxxLF motif with the LxxLF motif. SPEP-24 has an IC₅₀ of 5 nM, 5-fold better than SPEP-10, the most potent compound in the FxxLF series. The LxxLL motifs of SPEP-23 and SPEP-26 have IC₅₀s of 20 and 30 nM, respectively, comparable to SPEP-10.

Derivatization for Enhanced Cell Permeability

The presence of charged residues in SPEP-10 (SEKFAALFQSY) sequence may hinder the compound's penetration through the plasma membrane, as the AR is located first in the cytoplasm and then translocates to the nucleus upon ligand binding. Therefore, a number of substitutions were made in AF-2 peptide sequence, aimed to enhance membrane permeability of the compounds. We generated four less polar analogs (SPEP-25, SPEP-29, SPEP-35, and SPEP-36) of SPEP-10 by replacing either the glutamate or lysine residue with an uncharged one (Table 1). SPEP-20, SPEP-25, SPEP-29, SPEP-35, and SPEP-36 did not show equivalent or better potency (IC₅₀s of 200, 800, 500, and 75 nM, respectively) of binding vs. the parent compound SPEP-10. However, it was

Table 1 Composition of bivalent ligands

Compound	Androgen	Linker	AF-2 peptide
Linker length			
SPEP-1	DHT	GGGGG	SSRFGSLFAG
SPEP-2	DHT	GGGGGG	SSRFGSLFAG
SPEP-3	DHT	GGGG	SSRFGSLFAG
SPEP-9	DHT	GGGG GGGGGG	SEKFAALFQSY
Modified FXXLF			
SPEP-4	DHT	GGGGG	SEKFQNLFQSY
SPEP-5	DHT	GGGGG	SEKFAALFQSY
SPEP-6	DHT	GGGGG	SEKFKLLFQSY
γ -Abu-Ahx			
SPEP-10	DHT	G- γ -Abu-Ahx	SEKFAALFQSY
SPEP-27	DHT	G- γ -Abu-Ahx	SEKFKLLFQSY
Unnatural amino acids in AF-2 peptide			
SPEP-11	DHT	GGGGG	SEK-Cha-AALFQSY ¹
SPEP-12	DHT	GGGGG	SEKFAAL-Nal-QSY ²
SPEP-13	DHT	GGGGG	SEK-Cha-AAL-Nal-QSY
SPEP-19	DHT	G- γ -Abu-Ahx	SEK-Cha-AAL-Nal-QSY
SPEP-21	DHT	G- γ -Abu-Ahx	SEK-Nal-AAL-Nal-QSY
SPEP-22	DHT	G- γ -Abu-Ahx	SEK-Cha-AAL-Cha-QSY
XXLL motif			
SPEP-23	DHT	G- γ -Abu-Ahx	SEKLAALLQSY
SPEP-24	DHT	G- γ -Abu-Ahx	SEKLAALFQSY
SPEP-26	DHT	G- γ -Abu-Ahx	SHKLVQLLQSY
AF-2 peptide, reduced charge			
SPEP-20	DHT	G- γ -Abu-Ahx	SNQFAALFQSY
SPEP-25	DHT	G- γ -Abu-Ahx	SE-LYS(z)-FAALFQSY ³
SPEP-29	DHT	G- γ -Abu-Ahx	SQKFAALFQSY
SPEP-35	DHT	G- γ -Abu-Ahx	SEQFAALFQSY
SPEP-36	DHT	G- γ -Abu-Ahx	SNKFAALFQSY
Fatty acid			
SPEP-38	DHT	G- γ -Abu-Ahx	SEK(octanoic-acid)FAALFQSY
SPEP-41	DHT	G- γ -Abu-Ahx	SEK(hexanoic-acid)LAALFQSY
SPEP-42	DHT	G- γ -Abu-Ahx	SEK(octanoic-acid)LAALFQSY
SPEP-43	DHT	G- γ -Abu-Ahx	SEK(decanoic acid)LAALFQSY
Stapled AF-2 peptide			
HGSF-1	DHT	G- γ -Abu-Ahx	SEKFA <u>AALF</u> ASY ⁴
HGSF-2	DHT	G- γ -Abu-Ahx	SEKLA <u>AALF</u> ASY ⁴

¹ Cha, Cyclohexyl Alanine,

² Nal, Napthyl Alanine,

³ N- ϵ -benzyloxycarbonyl lysine

⁴ The underlined residues are the olefinic alanines that were stapled

observed that solubility of the compounds could be an issue in these series of compounds.

Another strategy to improve cell permeability is to derivatize the peptides with fatty acids. Fatty acids with different carbon chain lengths were attached to SPEP-10 and SPEP-24 through lysine side chain amino groups by peptide linkage

(Table 1). It is well known that medium chain fatty acids can enhance the cell permeability of certain drugs [51–53]. Molecular modeling suggested that incorporation of these fatty acids would not interfere with peptide binding. Therefore, hexanoic acid (SPEP-41), octanoic (SPEP-42, and decanoic acid (SPEP-43) derivatives of SPEP-24 were made and tested.

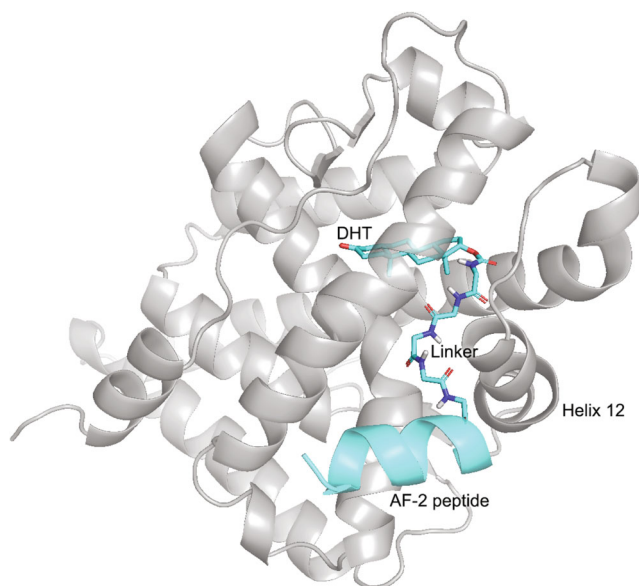


Fig. 2 Energy refined structure of steroid-peptide conjugate 1 (SPEP-1) bound to AR LBD. The steroid and glycine linker are represented as capped sticks and AF-2 peptide as a cyan ribbon. The AR LBD is represented as an ash colored ribbon. To help orient the view, helix 12 of AR is also labeled

These have in vitro IC_{50} values of 40, 50 and 25 nM, respectively. These are of lower affinity relative to SPEP-24 but still have respectable potency. SPEP-38 is an octanoic acid derivative of SPEP-10 and has an IC_{50} of 200 nM, an 8-fold decrease in potency, similar to the 5- to 10-fold decrease seen for the SPEP-24 derivatives.

Peptide Stapling

A number of structural analyses of AR-cofactor interactions shows that the FxxLF motif binds as a short helix located between a charge clamp at a fixed position of the AR AF-2 [45]. This helical structure is crucial to properly position the AF-2 peptide side chains for optimal binding. Our AF-2 peptide moiety is based on a short 11-residue fragment extracted from a larger domain. This short peptide, in the absence of the larger domain, may have a reduced helical stability, compromising its binding ability and also making it more prone to proteolytic digestion. Peptide stapling is a technique that locks a peptide in its rigid α -helical form, helping preserve its structural integrity and intermolecular interactions [54–59] (Fig. 4). Furthermore, preserving the intramolecular hydrogen bonding in the helix reduces the polar exposure of the amide backbone, thereby reducing the barrier to membrane penetration and increasing its resistance to protease cleavage. Typically, the amino acids to be linked are replaced by unnatural amino acids such as (*S*)-2-(2-pentenyl) alanine whose side chains are then cross-linked with an olefinic bond. The AF-2 peptides are two-turn amphipathic α -helices. Molecular modeling suggested that an *i, i + 4* crosslink for

Table 2 In vitro cell-free binding assays

Compound	IC_{50} (nM) ¹	K_i (nM) ²
SPEP-1 #	500	115.5
SPEP-2	-	-
SPEP-3	-	-
SPEP-4 #	300	69
SPEP-5*#	70	16
SPEP-6 #	100	23
SPEP-9 #	100	23
SPEP-10*#	26	6
SPEP-11	300	69
SPEP-12	200	46
SPEP-13	100	23
SPEP-19	200	46
SPEP-21 #	500	115
SPEP-22 #	700	162
SPEP-23 #	20	4
SPEP-24*#	5	1
SPEP-25 #	200	46
SPEP-26*#	30	7
SPEP-27*	50	11
SPEP-29	800	185
SPEP-35	500	115
SPEP-36*	75	17
SPEP-38	200	46
SPEP-41*	40	9
SPEP-42*	50	11
SPEP-43*	25	6
HGSF-1*#	5	1
HGSF-2*#	2	0.5

¹ IC_{50} calculated as the concentration required to compete 50% of [³H] MB binding. -, no competition

² $K_i = IC_{50}$ of the compound/(1 + Conc. of MB in the assay/ K_d of MB³)

³ K_d of MB is 1.5 nM [49]

*Compounds that were selected for cell culture inhibition assay (see Table 3)

Kinetic binding assays are provided in Supplemental Data 1, for selected compounds

the olefinic alanines replacing the underlined A and Q amino acids in the AF-2-binding peptides, SEKFAAALFQSY and SEKLAAALFQSY, are not expected to interfere with AR binding. The olefinic amino acids are on the solvent-exposed face of the α -helix. The two stapled peptides (HGSF-1 and HGSF-2) were made and tested. HGSF-1 is a stapled version of SPEP-10 and has an in vitro IC_{50} of 5 nM, a 5-fold improvement over SPEP-10. HGSF-2 is a stapled version of SPEP-24 and has an IC_{50} of 2 nM, a 2.5-fold improvement. These results are supportive of the ability to design constrained fragments of known structural motifs that can affect critical protein-protein binding interactions as AR and co-activator

peptide interactions, and possibly why they are considerably more potent than the unconstrained LxxLF motif.

In Vivo Binding

Eleven compounds with good in vitro binding (less than 100 nM) to AR were checked for their in vivo affinity for AR (Table 3) by competing for binding against synthetic [³H]-labeled androgen mibolerone in a genital skin fibroblast assay. The most potent ligands were SPEP-24 and SPEP-36, with 90 and 91% inhibition, respectively. SPEP-36 is 15-fold weaker than SPEP-24 in vitro but has comparable potency in vivo. This may be due to greater cell permeability of SPEP-36 resulting from mutating a charged glutamate to a neutral asparagine residue. Despite the good in vitro potency of the stapled peptides, in vivo potency was relatively weak. It is possible that the stapled peptides may have reduced cell permeability.

Molecular Dynamics Simulation

Figure 2 shows the energy-minimized structure of the complex of AR and SPEP-1. The introduction of the Gly₅ linker is accommodated with relatively small adjustments in the AR structure. To further assess whether the designed bivalent conjugates would seriously perturb the structural integrity of the AR protein a 50-ns molecular dynamics simulation was carried out on SPEP-24, one of the designed conjugates that exhibited good binding in both in vitro and cellular assays. A stereoscopic snapshot of the structure of the complex of AR with SPEP-24 taken towards the end of the 50-ns MD

simulation is shown in Fig. 3a. Superposition onto the crystal structure of AR with DHT and the AF-2 peptide (pdb code 1t7r) shows that the AR structure is not significantly perturbed, and the AF-2 peptide binding mode and helical structure is preserved. The integrity of helix 12 in AR is also maintained, albeit translated somewhat. Figure 3b shows a more detailed view of the interactions of the AF-2 motif with its binding site on AR. We see that tethering the AF-2 peptide to the steroid does not compromise its ability to bind to AR and can thus contribute to the overall binding affinity of the bivalent ligand. The hydrophobic groups in the LxxLF motif (labeled + 1, + 4 and + 5 in Fig. 3b) all point towards the AR and are buried. The leucine side chain at position + 1 interacts with I737 at the bottom of the binding site groove and is sandwiched by L712 and M734 at the sides of the groove. The leucine side chain at + 4 packs against L712, V713, and V716 in a relatively shallow binding region. The phenylalanine side chain at + 5 is buried deeply at the other end of the binding groove and is sandwiched between the aliphatic

Table 3 Cell-based binding assay

Compound	% competition of [³ H] MB binding ¹
[³ H] MB	82
SPEP-5	57
SPEP-10	67
SPEP-19	82
SPEP-22	85
SPEP-24	90
SPEP-26	73
SPEP-27	71
SPEP-36	91
SPEP-41	50
SPEP-42	31
SPEP-43	73
HGSF-1	10
HGSF-2	40

¹ Percent inhibition of MB binding in cultured cell (2080 genital skin fibroblast, GSF) assay; conjugate concentration 500 nM, except for SPEP-24, which was at 50 nM

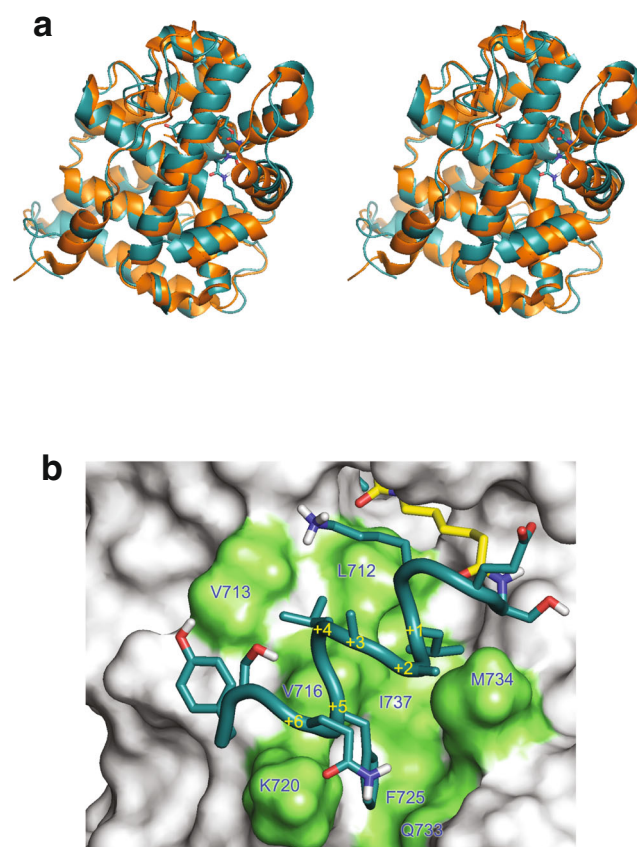
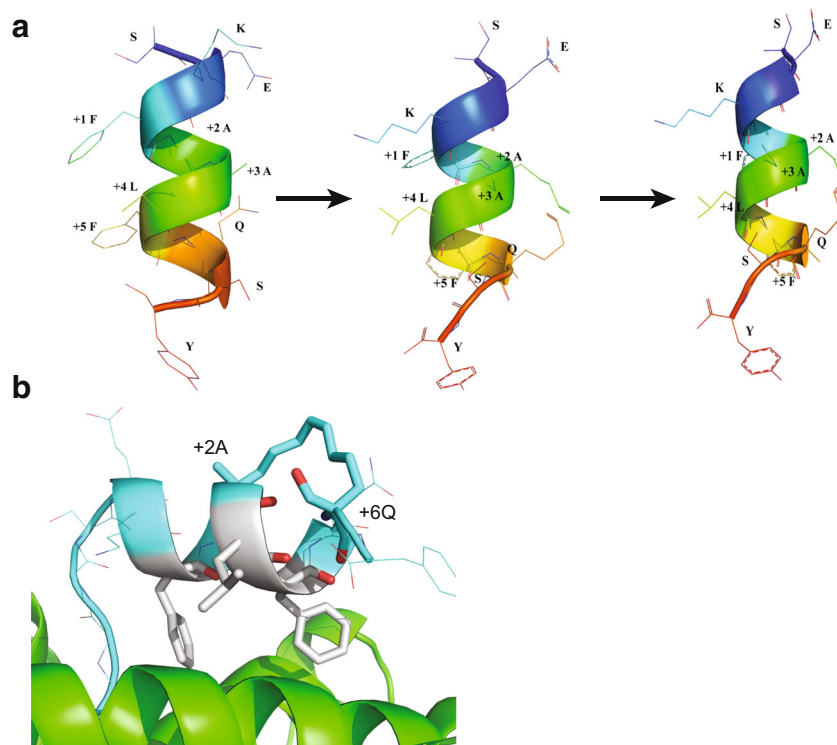


Fig. 3 Complex of AR and SPEP-24. **a** A stereoscopic snapshot of the complex of AR and SPEP-24 taken towards the end of the 50-ns MD simulation. The orientation of the complex is similar to that in Fig. 2. SPEP-24 is in teal with the steroid and linker represented as sticks. All other residues are represented as ribbons. Overlaid in orange is the crystal structure of a complex of AR, DHT, and an AF-2 peptide. **b** Detailed view of the interactions of the AF-2 peptide with AR. The ligand is represented with capped sticks and the AR LBD as a molecular surface. The LxxLF motif is labeled from + 1 to + 5

Fig. 4 Strategy adopted for stapled AF-2 peptides. **a** Cross-linked pentenylalanines replacing the +2 A (n) and +6 Q ($n+4$) in SEKFAALFQAY. **b** Interaction of HGSF-1 with the AF-2 of AR. The stapled peptide HGSF-1 are displayed as sticks (cyan) and AF-2 surface displayed as molecular surface (green). The stapled side chains are all solvent-exposed



carbons of the K720 and the side chain of Q733 as well as interacting with F725 at the bottom of the groove. The modeled structure also shows that the +2 and +6 positions point to solvent and are compatible with peptide stapling in HGSF-1 and HGSF-2 (Table 1, Fig. 4). The DHT-bivalent SPEP-24 compound interaction complex appears to have equilibrated from 30 ns onwards to a structure with a backbone root-mean-square deviation (RMSD) of 1.7 Å from the crystal structure of AR (Fig. 5). This suggests that the

introduction of the bivalent compound does not significantly perturb the structure of the AR LBD. As a control, a molecular dynamics simulation was also carried out for crystal structure of AR with DHT alone and a similar RMSD of 1.6 Å from the initial structure was observed.

Conclusions

We have designed bivalent ligands of AR that utilize both the steroid and AF-2 binding sites. This was made possible by linking the two sites through a hitherto unrecognized nascent channel that is readily enlarged to accommodate a Gly₅ linker (or the isosteric Gly-γ-Abu-Ahx peptidomimetic) with minimal perturbation of the protein structure. The most active of these ligands exhibited single-digit nanomolar IC₅₀s in vitro. Moreover, some of these ligands retained good activity in cellular assays with up to 90% inhibition of mibolerone binding. The goal of this work was not to create androgen antagonists per se but rather to create potent and specific targeting agents that could eventually carry a cytotoxic payload. For example, the C-terminal Tyr in the ligand facilitates the introduction of radioactive iodine-131. The AF-2 binding moiety provides other solvent-exposed side chain positions that could be derivatized to incorporate photodynamic agents or other cytotoxic agents. Previous attempts at using the steroid alone as the targeting moiety to which a cytotoxic agent is attached have had limited success [36]. For example, an androgen-mustard conjugate, where 2-chloroethyl aniline is connected

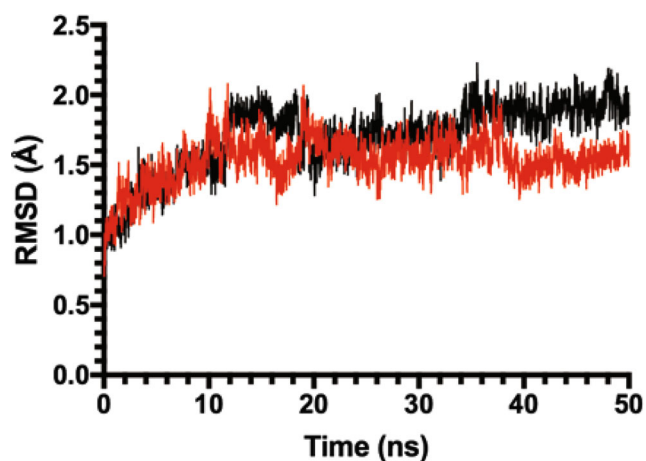


Fig. 5 Structural dynamics of the bound AR-LBD and SPEP-24 complex. In black is the root-mean-square deviation (RMSD) along the molecular dynamics trajectory of all backbone atoms of AR LBD in complex with SPEP-24 with respect to the crystal structure of DHT and an AF-2 peptide bound to AR-LBD (pdb code 1t7r). In red is the corresponding plot for a molecular dynamics simulation for AR-LBD with DHT alone

to an 8-carbon atom linker at the substitution-tolerant C₁₁ position of the androgen methyltrienolone (R1881), shows extensive cytotoxic properties, but with one-tenth the binding affinity of natural androgens, resulting in an unacceptable level of systemic toxicity [36]. The greater affinity of the bivalent ligand developed in this work could alleviate the problem of systemic toxicity for delivering cytotoxic agents. Therefore, the functionality of the modified compound-AR complex (i.e., agonist or antagonist activity) is not relevant; the vital parameter is its ability to deliver toxic agents or sensitizers to the tumorigenic cells. One of the advantages of choosing the AR and its ligands as a target system is the large amount of structural information available for the AR ligand-binding domain. All modalities listed above would incorporate active moieties that are extremely small, allowing for good access to cytoplasmic ARs.

The use of any present-day cancer therapeutics is likely to falter because of the uncanny ability of cancers to become resistant to such treatments. We propose that a different approach is needed, i.e., delivery of toxic physical modalities or sensitizers (drug/pro-drugs) not susceptible to biological resistance. Such de novo therapeutic agents require much improved targeting techniques. Prostate tissue and PCa have relatively high AR content (approximately 400 fmol/mg protein) [60]. Indeed, although the AR is expressed in other male reproductive organs, kidney, liver, and certain areas of the central nervous system, ¹⁸F-labeled-DHT given systemically targets prostate tissue [61–64]; similarly, these bivalent compounds should do the same. Therefore, the bivalent ligands described here were developed specifically to target AR, with a similar strategy that could be pursued with other members of the steroid receptor family [41, 42]. Thus, the potential for toxicity in other tissues expressing AR is possible if the targeted active agents are directly toxic, but not so if the non-biological targeted agents are delivered as a pro-drug or sensitizer, i.e., a second modality that can also be targeted to the prostate is required to activate the pro-drug. Classical antagonists certainly can be seen to be ineffective in such cases, because they are required to “operate” within the cellular environment, as are most chemotherapeutics. Thus, cells with early somatic changes, rendering them resistant to the proposed therapy, or cells where AR expression is lost, can still be exposed to toxins delivered to the near-by environment. Cells devoid of the AR are unlikely to be affected. However, non-biological agents typically do not require a cellular environment to be effective and can be effective beyond the single host cell. A “radius effect” is commonly seen. The best example would be radioactive iodine-131 (¹³¹I), used in the treatment of thyroid cancer, where beta emission has been well documented to kill cells in a microenvironment, even though not all cells take up iodine. Moreover, this work may have much broader implications, as any neoplastic tissue harboring a sufficient concentration of a steroid receptor may be

amendable to effective treatment employing compounds targeted to their respective receptors.

Funding Information The work was supported by a grant from Prostate Cancer Canada/Movember Foundation—Pilot Grant (#2012-905). Salary support for S.C. was provided by The Department of Urology—Jewish General Hospital (Montreal, Canada).

Publisher’s Note Springer Nature remains neutral with regard to jurisdictional claims in published maps and institutional affiliations.

References

- Kobayashi T, Kamba T, Terada N, Yamasaki T, Inoue T, Ogawa O (2016) High incidence of urological complications in men dying from prostate cancer. *Int J Clin Oncol* 21(6):1150–1154
- Carlsson S, Drevin L, Loeb S, Widmark A, Lissbrant IF, Robinson D, Johansson E, Stattin P, Fransson P (2016) Population-based study of long-term functional outcomes after prostate cancer treatment. *BJU Int* 117(6B):E36–E45
- Attard G et al (2016) Prostate cancer. *Lancet* 387(10013):70–82
- Torre LA et al (2015) Global cancer statistics, 2012. *CA Cancer J Clin* 65(2):87–108
- DePriest AD et al (2016) Regulators of androgen action resource: a one-stop shop for the comprehensive study of androgen receptor action. *Database*
- Beltran H et al (2016) Emerging molecular biomarkers in advanced prostate cancer: translation to the clinic. *Am Soc Clin Oncol Educ Book* 35:131–141
- Katsogiannou M, Ziouziou H, Karaki S, Andrieu C, Henry de Villeneuve M, Rocchi P (2015) The hallmarks of castration-resistant prostate cancers. *Cancer Treat Rev* 41(7):588–597
- He B, Gampe RT Jr, Kole AJ, Hnat AT, Stanley TB, An G, Stewart EL, Kalman RI, Minges JT, Wilson EM (2004) Structural basis for androgen receptor interdomain and coactivator interactions suggests a transition in nuclear receptor activation function dominance. *Mol Cell* 16(3):425–438
- Bourguet W, Germain P, Gronemeyer H (2000) Nuclear receptor ligand-binding domains: three-dimensional structures, molecular interactions and pharmacological implications. *Trends Pharmacol Sci* 21(10):381–388
- Li Y, Lambert MH, Xu HE (2003) Activation of nuclear receptors: a perspective from structural genomics. *Structure* 11(7):741–746
- Levenson AS, Jordan VC (1999) Selective oestrogen receptor modulation: molecular pharmacology for the millennium. *Eur J Cancer* 35(12):1628–1639
- Steinmetz AC, Renaud JP, Moras D (2001) Binding of ligands and activation of transcription by nuclear receptors. *Annu Rev Biophys Biomol Struct* 30:329–359
- Estebanez-Perpina E et al (2005) The molecular mechanisms of coactivator utilization in ligand-dependent transactivation by the androgen receptor. *J Biol Chem* 280(9):8060–8068
- Gronemeyer H, Gustafsson JA, Laudet V (2004) Principles for modulation of the nuclear receptor superfamily. *Nat Rev Drug Discov* 3(11):950–964
- Isaacs JT, Isaacs WB (2004) Androgen receptor outwits prostate cancer drugs. *Nat Med* 10(1):26–27
- Robinson D, van Allen EM, Wu YM, Schultz N, Lonigro RJ, Mosquera JM, Montgomery B, Taplin ME, Pritchard CC, Attard G, Beltran H, Abida W, Bradley RK, Vinson J, Cao X, Vats P, Kunju LP, Hussain M, Feng FY, Tomlins SA, Cooney KA, Smith DC, Brennan C, Siddiqui J, Mehra R, Chen Y, Rathkopf DE, Morris MJ, Solomon SB, Durack JC, Reuter VE, Gopalan A, Gao J, Loda

- M, Lis RT, Bowden M, Balk SP, Gaviola G, Sougnez C, Gupta M, Yu EY, Mostaghel EA, Cheng HH, Mulcahy H, True LD, Plymate SR, Dvinge H, Ferraldeschi R, Flohr P, Miranda S, Zafeiriou Z, Tunariu N, Mateo J, Perez-Lopez R, Demichelis F, Robinson BD, Schiffman M, Nanus DM, Tagawa ST, Sigaras A, Eng KW, Elemento O, Sboner A, Heath EI, Scher HI, Pienta KJ, Kantoff P, de Bono JS, Rubin MA, Nelson PS, Garraway LA, Sawyers CL, Chinnaiyan AM (2015) Integrative clinical genomics of advanced prostate cancer. *Cell* 161(5):1215–1228
17. Schroder F et al (2012) Androgen deprivation therapy: past, present and future. *BJU Int* 109(Suppl 6):1–12
 18. Zaman N et al (2014) Proteomic-coupled-network analysis of T877A-androgen receptor interactomes can predict clinical prostate cancer outcomes between White (non-Hispanic) and African-American groups. *PLoS One* 9(11):e113190
 19. Sun C, Shi Y, Xu LL, Nageswararao C, Davis LD, Segawa T, Dobi A, McLeod DG, Srivastava S (2006) Androgen receptor mutation (T877A) promotes prostate cancer cell growth and cell survival. *Oncogene* 25(28):3905–3913
 20. Robins DM (2012) Androgen receptor gene polymorphisms and alterations in prostate cancer: of humanized mice and men. *Mol Cell Endocrinol* 352(1–2):26–33
 21. Gottlieb B et al (2012) The androgen receptor gene mutations database: 2011 update. *Hum Mutat*
 22. Duff J, McEwan IJ (2005) Mutation of histidine 874 in the androgen receptor ligand-binding domain leads to promiscuous ligand activation and altered p160 coactivator interactions. *Mol Endocrinol* 19(12):2943–2954
 23. Korpai M, Korn JM, Gao X, Rakiec DP, Ruddy DA, Doshi S, Yuan J, Kovats SG, Kim S, Cooke VG, Monahan JE, Stegmeier F, Roberts TM, Sellers WR, Zhou W, Zhu P (2013) An F876L mutation in androgen receptor confers genetic and phenotypic resistance to MDV3100 (enzalutamide). *Cancer discovery* 3(9):1030–1043
 24. Bill-Axelson A, Holmberg L, Garmo H, Rider JR, Taari K, Busch C, Nordling S, Häggman M, Andersson SO, Spångberg A, Andrén O, Palmgren J, Steineck G, Adami HO, Johansson JE (2014) Radical prostatectomy or watchful waiting in early prostate cancer. *N Engl J Med* 370(10):932–942
 25. Wilt TJ, Brawer MK, Jones KM, Barry MJ, Aronson WJ, Fox S, Gingrich JR, Wei JT, Gilhooly P, Grob BM, Nsouli I, Iyer P, Cartagena R, Snider G, Roehrborn C, Sharifi R, Blank W, Pandya P, Andriole GL, Culkin D, Wheeler T (2012) Radical prostatectomy versus observation for localized prostate cancer. *N Engl J Med* 367(3):203–213
 26. Bill-Axelson A, Holmberg L, Filen F, Ruutu M, Garmo H, Busch C, Nordling S, Häggman M, Andersson SO, Bratell S, Spångberg A, Palmgren J, Adami HO, Johansson JE, for the Scandinavian Prostate Cancer Group Study Number 4 (2008) Radical prostatectomy versus watchful waiting in localized prostate cancer: the Scandinavian prostate cancer group-4 randomized trial. *J Natl Cancer Inst* 100(16):1144–1154
 27. Case DA, Cheatham TE, Darden T, Gohlke H, Luo R, Merz KM, Onufriev A, Simmerling C, Wang B, Woods RJ (2005) The Amber biomolecular simulation programs. *J Comput Chem* 26(16):1668–1688
 28. Hornak V, Abel R, Okur A, Strockbine B, Roitberg A, Simmerling C (2006) Comparison of multiple Amber force fields and development of improved protein backbone parameters. *Proteins: Struct Funct Bioinf* 65(3):712–725
 29. Wang J, Wolf RM, Caldwell JW, Kollman PA, Case DA (2004) Development and testing of a general amber force field. *J Comput Chem* 25(9):1157–1174
 30. Darden T, York D, Pedersen L (1993) Particle mesh Ewald: an $N \log(N)$ method for Ewald sums in large systems. *J Chem Phys* 98(12):10089–10092
 31. Ryckaert JP, Ciccotti G, Berendsen HJC (1977) Numerical integration of the cartesian equations of motion of a system with constraints: molecular dynamics of n-alkanes. *J Comput Phys* 23(3):327–341
 32. Hauptmann H, Metzger J, Schnitzbauer A, Cuilleron CY, Mappus E, Luppia PB (2003) Syntheses and ligand-binding studies of 1 alpha- and 17 alpha-aminoalkyl dihydrotestosterone derivatives to human sex hormone-binding globulin. *Steroids* 68(7–8):629–639
 33. Ngatcha BT, Luu V (2000) The, and D. Poirier, Androstereone 3beta-substituted derivatives as inhibitors of type 3 17beta-hydroxysteroid dehydrogenase. *Bioorg Med Chem Lett* 10(22):2533–2536
 34. Kim YW, Grossmann TN, Verdine GL (2011) Synthesis of all-hydrocarbon stapled alpha-helical peptides by ring-closing olefin metathesis. *Nat Protoc* 6(6):761–771
 35. Shkolny DL et al (1999) Discordant measures of androgen-binding kinetics in two mutant androgen receptors causing mild or partial androgen insensitivity, respectively. *J Clin Endocrinol Metab* 84(2):805–810
 36. Marquis JC, Hillier SM, Dinaut AN, Rodrigues D, Mitra K, Essigmann JM, Croy RG (2005) Disruption of gene expression and induction of apoptosis in prostate cancer cells by a DNA-damaging agent tethered to an androgen receptor ligand. *Chem Biol* 12(7):779–787
 37. Schaschke N, Dominik A, Matschiner G, Sommerhoff CP (2002) Bivalent inhibition of beta-tryptase: distance scan of neighboring subunits by dibasic inhibitors. *Bioorg Med Chem Lett* 12(6):985–988
 38. Selwood T, Smolensky H, McCaslin DR, Schechter NM (2005) The interaction of human tryptase-beta with small molecule inhibitors provides new insights into the unusual functional instability and quaternary structure of the protease. *Biochemistry* 44(9):3580–3590
 39. Slon-Usakiewicz JJ, Sivaraman J, Li Y, Cygler M, Konishi Y (2000) Design of P1' and P3' residues of trivalent thrombin inhibitors and their crystal structures. *Biochemistry* 39(9):2384–2391
 40. Slon-Usakiewicz JJ, Purisima E, Tsuda Y, Sulea T, Pedyczak A, Féthière J, Cygler M, Konishi Y (1997) Nonpolar interactions of thrombin S' subsites with its bivalent inhibitor: methyl scan of the inhibitor linker. *Biochemistry* 36(44):13494–13502
 41. Shan M, Bujotzek A, Abendroth F, Wellner A, Gust R, Seitz O, Weber M, Haag R (2011) Conformational analysis of bivalent estrogen receptor ligands: from intramolecular to intermolecular binding. *Chembiochem* 12(17):2587–2598
 42. Shan M, Carlson KE, Bujotzek A, Wellner A, Gust R, Weber M, Katzenellenbogen JA, Haag R (2013) Nonsteroidal bivalent estrogen ligands: an application of the bivalent concept to the estrogen receptor. *ACS Chem Biol* 8(4):707–715
 43. Heery DM, Kalkhoven E, Hoare S, Parker MG (1997) A signature motif in transcriptional co-activators mediates binding to nuclear receptors. *Nature* 387(6634):733–736
 44. AgoulNIK IU, Weigel NL (2008) Androgen receptor coactivators and prostate cancer. *Horm Carci* V 617:245–255
 45. Hur E, Pfaff SJ, Payne ES, Grøn H, Buehrer BM, Fletterick RJ (2004) Recognition and accommodation at the androgen receptor coactivator binding interface. *PLoS Biol* 2(9):E274
 46. Li X, Martinez-Ferrer M, Botta V, Uwamariya C, Banerjee J, Bhowmick NA (2011) Epithelial Hic-5/ARA55 expression contributes to prostate tumorigenesis and castrate responsiveness. *Oncogene* 30(2):167–177
 47. Miyamoto H, Rahman M, Takatera H, Kang HY, Yeh S, Chang HC, Nishimura K, Fujimoto N, Chang C (2002) A dominant-negative mutant of androgen receptor coregulator ARA54 inhibits androgen receptor-mediated prostate cancer growth. *J Biol Chem* 277(7):4609–4617

48. Thin TH, Wang L, Kim E, Collins LL, Basavappa R, Chang C (2003) Isolation and characterization of androgen receptor mutant, AR(M749L), with hypersensitivity to 17-beta estradiol treatment. *J Biol Chem* 278(9):7699–7708
49. Murthy LR, Johnson MP, Rowley DR, Young CYF, Scardino PT, Tindall DJ (1986) Characterization of steroid receptors in human prostate using mibolerone. *Prostate* 8(3):241–253
50. Fletterick RJ (2005) Molecular modelling of the androgen receptor axis: rational basis for androgen receptor intervention in androgen-independent prostate cancer. *BJU Int* 96:2–9
51. Artursson P (1998) Application of physicochemical properties of molecules to predict intestinal permeability. In *Proceedings of the AAPS Workshop on Permeability Definitions and Regulatory Standards*. Arlington, VA
52. Guharoy M, Chakrabarti P (2007) Secondary structure based analysis and classification of biological interfaces: identification of binding motifs in protein-protein interactions. *Bioinformatics* 23(15):1909–1918
53. Wagstaff KM, Jans DA (2006) Protein transduction: cell penetrating peptides and their therapeutic applications. *Curr Med Chem* 13(12):1371–1387
54. Bernal F, Tyler AF, Korsmeyer SJ, Walensky LD, Verdine GL (2007) Reactivation of the p53 tumor suppressor pathway by a stapled p53 peptide. *J Am Chem Soc* 129(9):2456–2457
55. Bhattacharya S, Zhang H, Debnath AK, Cowburn D (2008) Solution structure of a hydrocarbon stapled peptide inhibitor in complex with monomeric C-terminal domain of HIV-1 capsid. *J Biol Chem* 283(24):16274–16278
56. Henchey LK, Jochim AL, Arora PS (2008) Contemporary strategies for the stabilization of peptides in the alpha-helical conformation. *Curr Opin Chem Biol* 12(6):692–697
57. Leduc AM, Trent JO, Wittliff JL, Bramlett KS, Briggs SL, Chirgadze NY, Wang Y, Burris TP, Spatola AF (2003) Helix-stabilized cyclic peptides as selective inhibitors of steroid receptor-coactivator interactions. *Proc Natl Acad Sci U S A* 100(20):11273–11278
58. Walensky LD et al (2004) Activation of apoptosis in vivo by a hydrocarbon-stapled BH3 helix. *Science* 305(5689):1466–1470
59. Walensky LD, Pitter K, Morash J, Oh KJ, Barbuto S, Fisher J, Smith E, Verdine GL, Korsmeyer SJ (2006) A stapled BID BH3 helix directly binds and activates BAX. *Mol Cell* 24(2):199–210
60. Linja MJ et al (2001) Amplification and overexpression of androgen receptor gene in hormone-refractory prostate cancer. *Cancer Res* 61(9):3550–3555
61. Beattie BJ et al (2010) Pharmacokinetic assessment of the uptake of 16beta-18F-fluoro-5alpha-dihydrotestosterone (FDHT) in prostate tumors as measured by PET. *J Nucl Med* 51(2):183–192
62. Dehdashti F, Picus J, Michalski JM, Dence CS, Siegel BA, Katzenellenbogen JA, Welch MJ (2005) Positron tomographic assessment of androgen receptors in prostatic carcinoma. *Eur J Nucl Med Mol Imaging* 32(3):344–350
63. Zanzonico PB et al (2004) PET-based radiation dosimetry in man of 18F-fluorodihydrotestosterone, a new radiotracer for imaging prostate cancer. *J Nucl Med* 45(11):1966–1971
64. Larson SM et al (2004) Tumor localization of 16beta-18F-fluoro-5alpha-dihydrotestosterone versus 18F-FDG in patients with progressive, metastatic prostate cancer. *J Nucl Med* 45(3):366–373